TECHNICAL ARTICLE

Propagation of cutaneous thermal injury: A mathematical model

Chuan Xue, PhD[1,2]*; Ching-Shan Chou, PhD[1,2]*; Chiu-Yen Kao, PhD[1,2,3]; Chandan K. Sen, PhD[1,4]; Avner Friedman, PhD[1,2]

1. Mathematical Biosciences Institute, The Ohio State University, Columbus, Ohio
2. Department of Mathematics, The Ohio State University, Columbus, Ohio
3. Department of Mathematics and Computer Science, Claremont McKenna College, Claremont, California
4. The Comprehensive Wound Center and Department of Surgery and Davis Heart and Lung Research Institute, The Ohio State University, Columbus, Ohio

Reprint requests:
Dr. Chuan Xue, Mathematical Biosciences Institute and Department of Mathematics, The Ohio State University, Columbus, OH 43210, USA.
Tel: 614 292 7236;
Fax: 614 292 1479;
Email: cxue@math.osu.edu

Dr. Ching-Shan Chou, Mathematical Biosciences Institute and Department of Mathematics, The Ohio State University, Columbus, OH 43210, USA.
Tel: 614 292 9947;
Fax: 614 292 1479;
Email: chou@math.osu.edu

*The first two authors contributed equally.

Manuscript received: February 3, 2011
Accepted in final form: September 21, 2011

DOI:10.1111/j.1524-475X.2011.00759.x

ABSTRACT

Cutaneous burn wounds represent a significant public health problem with 500,000 patients per year in the USA seeking medical attention. Immediately after skin burn injury, the volume of the wound burn expands due to a cascade of chemical reactions, including lipid peroxidation chain reactions. Such expansion threatens life and is therefore highly clinically significant. Based on these chemical reactions, the present paper develops for the first time a three-dimensional mathematical model to quantify the propagation of tissue damage within 12 hours post initial burn. We use the model to investigate the effect of supplemental antioxidant vitamin E for intercepting propagation. We show, for example, that if tissue levels of vitamin E tocotrienol are increased, postburn, by five times then this would slow down the lipid peroxide propagation by at least 50%. We chose the alpha-tocotrienol form of vitamin E as it is a potent inhibitor of 12-lipoxygenase, which is known to propagate oxidative lipid damage. Our model is formulated in terms of differential equations, and sensitivity analysis is performed on the parameters to ensure the robustness of the results.

According to the American Burn Association, 500,000 patients per year in the USA seek medical attention for burn injuries. Skin burns are classified as superficial or first-degree burns (epidermal damage only), partial-thickness or second-degree burns (dermal injury), full-thickness or third-degree burns (destruction also of the subcutaneous layer which contains the hair follicles, sweat glands, and the region where new skin cells are formed), and fourth-degree burns which extends to the underlying tissue of ligaments and muscles. The current clinical care for severely burned patients is intravenous fluid resuscitation, controlling infection, and scar-reducing surgical intervention.[1] Tissue damage, which can be characterized by the level of lipid peroxidation,[2] typically increases during the 24 hours after the initial burn. It is currently challenging for burn care providers to estimate the spatial distribution of lipid peroxidation in the burned tissue, in order to determine quantitatively the size and depth of the propagating damage.

For a partial-thickness cutaneous burn injury, lipid peroxide and related reactive species are mainly produced through the chain reaction of lipid peroxidation.[3–9] The chain reaction is initiated by the excessive reactive oxygen species (ROS), such as the hydroxyl radical ($^{\bullet}OH$), generated by heat acting upon lipid-rich skin tissue. The $^{\bullet}OH$ combines with a hydrogen atom in a lipid molecule and makes a lipid radical ($L^{\bullet}$) and water. The $L^{\bullet}$ is very unstable and quickly reacts with oxygen to produce a lipid peroxyl radical ($LOO^{\bullet}$). The $LOO^{\bullet}$ is also unstable and reacts with free lipid to make lipid peroxide (LOOH) and another free $L^{\bullet}$. What follows is a chain reaction involving several radical species and the production of lipid peroxidation chain reaction. In this process, the initial burn wound propagates and its propagation can be, for practical purposes, traced by the relatively stable byproducts of lipid peroxidation.[2,10,11] Such propagation may terminate under a number of conditions resulting in neutralization of ROS.[12–18] This may happen when lipid-phase antioxidant molecules intercept and terminate lipid peroxidation. One such effective lipid-phase antioxidant is vitamin E.[19–22] Vitamin E can be depleted during a burn, and supplementary vitamin E has been indicated as a potential rescue for burn.[23–26] The infiltrating leukocytes also produce free radicals that initiate lipid peroxidation, and this normally occurs about 12 hours after the initial injury.[27]

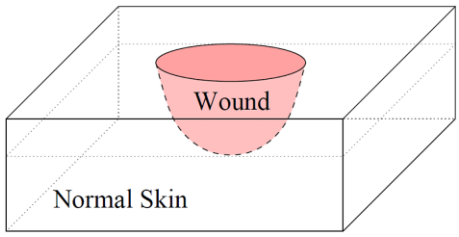

Figure 1. The three-dimensional geometry of a partial-thickness burn. The pink region represents the burnt wound that is surrounded by normal skin.

Mathematical modeling can be useful to determine the propagation of oxidative lipid damage in the tissue after a burn injury, thus helpful to quantify the extent of damage. Skin burn injury by surface heating or radiation was mathematically described.[28–30] These models are formulated in terms of the heat equation in the tissue, and do not include the chemical processes that result in the lipid peroxide propagation.

In this paper, we develop, for the first time, a mathematical mechanistic model to quantify the extent of the burn propagation after the initial damage, based on the passive biochemical events that are involved in the lipid peroxidation chain reaction initiated by the heat insult of lipid-rich skin tissue. Other enzymatic processes are involved in the origin and fate of lipid peroxidation, for example, through superoxide dismutase, catalase, glutathione peroxidase, and metal ions.[6] These details are only implicitly included in the rate parameters of the chemical processes. As we are modeling the propagation of the burn only in the 12 hours from the initial burn, we do not include the infiltrating leukocytes (and resulting contribution to oxidative stress) which occur only at a later time. We show that simulation of the model in the case of comb burn qualitatively agrees with experimental results in Singer et al.[31] We also use the model to examine the relative effect of intervention using vitamin E with different doses on limiting propagation of cutaneous thermal injury. Our simulation results show that if the skin tissue loading of vitamin E is increased, postburn, by five times as can be achieved by topical delivery, then this would slow down the propagation of lipid peroxidation by at least 50%. We performed sensitivity analysis in order to determine the extent to which our results depend on uncertainty in the parameters; we identified the parameters which have strong effect on burn propagation, and, at the same time, established robustness of the model predictions within a specified range of the parameters.

MATERIALS AND METHODS

The lipid peroxidation chain reactions

We consider a partial-thickness burn wound as shown in Figure 1. The thickness of the epidermal layer typically varies from 0.5 to 1.5 mm and the thickness of the dermal layer varies from 0.5 to 3 mm, depending on the location of the burn wound on the human body. When a burn injury occurs, the heat insult initiates a cascade of chemical reactions.[3–9] Healthy lipids are converted to lipid peroxides in chemical processes that involve, respectively, $^{\bullet}OH$, lipid alkoxyl radical $LO^{\bullet}$, and $LOO^{\bullet}$. These three radicals are also produced by lipid peroxide, thereby enhancing lipid peroxide propagation. This network of chemical reactions is depicted schematically in Figure 2; the major chemical reactions and reaction rates are given in Table 1. The chemical reactions can be divided into four processes: initiation, propagation, branching, and termination. The propagation and branching are the primary processes responsible for the increase of the size of the burn. It is known that vitamin E breaks up the chain reaction by scavenging the $LOO^{\bullet}$ and by blocking 12-lipoxygenase which oxidizes unsaturated lipid to lipid peroxide.[6,32–34] In this paper, we first model the mechanism by which the wound enlarges, and then model the termination of this process by intervention with vitamin E.

Our mathematical model is described in Equations (1)–(8). We assume that the burn is instantaneous. The temperature field, which affects the cascade of the chemical reactions, will not be included in our model explicitly; instead, the damage by the high temperature of the burn is reflected by the initial conditions of the chemicals which reflect the damage done by the high temperature of the burn. In particular, reaction (1) occurs instantaneously at time 0, and provides the initial amount of reactive oxygen and lipid species. Reaction (15) listed in Table 1 is the pro-oxidant effect of vitamin E; as it happens on a much slower time scale than the other reactions, we shall neglect it. The species 12-lipoxygenase is only implicitly modeled through the inhibition of $LOO^{\bullet}$ by vitamin E. Normal lipid molecules diffuse within single cell membranes, but there is no evidence showing that lipid molecules transport from cell to cell; therefore, we neglect the diffusion of lipids in the burn tissue. As the time scale for the propagation of the burn is much smaller than the time scale for remodeling of the

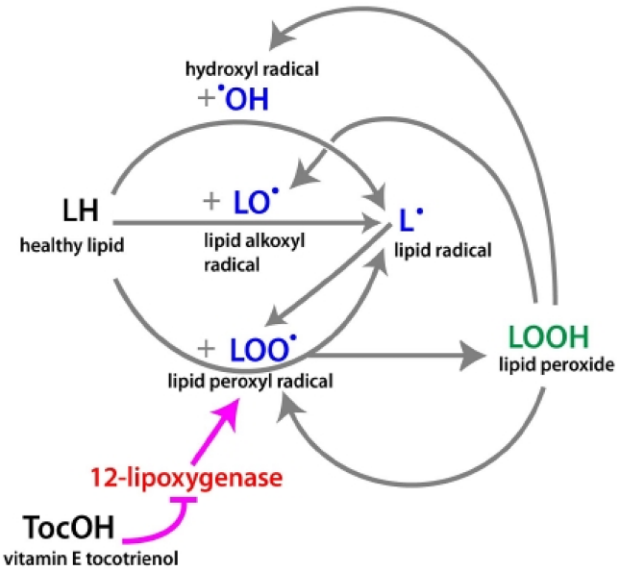

Figure 2. Network of the chemical reactions involved in burn propagation. Pointing arrows represent production of the chemicals, and barred arrow represents inhibition. The magenta colored arrows indicates pathway of the intervention by vitamin E tocotrienol.

Table 1. The chain reactions and reaction rates

Role		Reaction	Reaction rate	Reference
Initiation	(1)	$LH \rightarrow L^{\bullet}$	Heat or UV light, initial condition	
	(2)	$^{\bullet}OH + LH \xrightarrow{\lambda_2} L^{\bullet} + H_2O$	5×10^8 M^{-1} s^{-1}	36,37
Propagation	(3)	$L^{\bullet} + O_2 \xrightarrow{k_3/[O_2]} LOO^{\bullet}$	$3.0 - 4.6 \times 10^8$ M^{-1} s^{-1} Cellular $[O_2] = 1.0 \times 10^{-4}$ M	36 Table 2, 3,36, 6 p. 4
	(4)	$LOO^{\bullet} + LH \xrightarrow{\lambda_4} LOOH + L^{\bullet}$	19 M^{-1} s^{-1} (lipids with 2 double bonds)	36 Table 2
	(5)	$LO^{\bullet} + LH \xrightarrow{\lambda_5} NRP + L^{\bullet}$	1.0×10^7 M^{-1} s^{-1}	36 Table 2
Branching	(6)	$LOOH + Fe^{2+} \xrightarrow{k_6/[Fe^{2+}]} LO^{\bullet} + Fe^{3+} + OH^-$	1.5×10^3 M^{-1} s^{-1} $[Fe^{2+}] = 10^{-7}$ M	6 p. 246, 36
	(7)	$LOOH + Fe^{3+} \xrightarrow{k_7/[Fe^{3+}]} LOO^{\bullet} + Fe^{2+} + H^+$	Slower than above 10^3 M^{-1} s^{-1}	6 p.246, this work
	(8)	$LOOH \xrightarrow{k_8} LO^{\bullet} + OH^{\bullet}$	$k_6/20$	38 p. 185, 6 p. 246, this work
Termination	(9)	$2LOO^{\bullet} \xrightarrow{\lambda_9} NRP$	6.6×10^4 M^{-1} s^{-1}	36 Table 2
	(10)	$2L^{\bullet} \xrightarrow{\lambda_{10}} NRP$	6.6×10^4 M^{-1} s^{-1}	39,36 p. 941
	(11)	$2LO^{\bullet} \xrightarrow{\lambda_{11}} NRP$	6.6×10^4 M^{-1} s^{-1}	39,36 p. 941
	(12)	$L^{\bullet} + LOO^{\bullet} \xrightarrow{\lambda_{12}} NRP$	10^5 M^{-1} s^{-1}	38 p. 185, this work
Antioxidant	(13)	$LOO^{\bullet} + TocOH \xrightarrow{\lambda_{13}} TocO^{\bullet} + LOOH$	10^6 M^{-1} s^{-1}	6 p. 168
	(14)	$LOO^{\bullet} + TocO^{\bullet} \xrightarrow{\lambda_{14}} NRP$	2×10^4 M^{-1} s^{-1}	$\lambda_{12}/50$
	(15)	$TocO^{\bullet} + LH \longrightarrow L^{\bullet} + TocOH$	5×10^{-2} M^{-1} s^{-1}(slow)	6 p. 169

Notations are based on Figure 2, with additional notations: $TocO^{\bullet}$ (vitamin E radical), NRP (non-radical product), Fe^{2+} (ferrous ion), Fe^{3+} (ferric ion), OH^- (hydroxide ion), and H^+ (proton).

damaged vascular system, we do not consider, in our model, the vascular system and the immune response.

The mathematical model

Under the earlier assumptions, we derive, by the law of mass action and diffusion, the model Equations (1)–(8). This reaction–diffusion system will be complemented by initial conditions and boundary conditions for each species. Most of the parameters in Equations (1)–(8) are obtained (or calculated) from the literature (Tables 1 and 2), with a few approximated or estimated as described in the Supporting Information (SI). The model involves processes that occur on a huge range of time scales, from nanoseconds (chain

Table 2. Parameters that do not appear in Table 1 and their references

Notation	Parameter value	References and notes
$D_{LOO^{\bullet}}$	1.8×10^{-5} cm^2 h^{-1}	40,36 Table 5 and p. 927
D_{LOOH}	1.8×10^{-5} cm^2 h^{-1}	40,36 Table 5 and p. 927
D_{TocOH}	1.8×10^{-2} cm^2 h^{-1}	41,36 Table 5 and p. 927
$D_{TocO^{\bullet}}$	1.8×10^{-2} cm^2 h^{-1}	41,36 Table 5 and p. 927
$D_{^{\bullet}OH}$	1.8×10^{-2} cm^2 h^{-1}	36 Table 5 and p. 927
$D_{L^{\bullet}}$	1.8×10^{-5} cm^2 h^{-1}	40,36 Table 5 and p. 927
$D_{LO^{\bullet}}$	1.8×10^{-5} cm^2 h^{-1}	40,36 Table 5 and p. 927
L_0	2.5×10^{-2} M	About 10% of cell volume 3,36 represents the concentration of healthy lipid.
A_0	4×10^{-4} M	500 nmol/g (specific weight for fat is 0.8 g/mL) denotes the concentration of vitamin E in healthy skin
k_{a1}	1.4×10^{-4} M h^{-1}	Basal $k_{a1} = \mu_a A_0$
k_{a2}		depends on the treatment
μ_a	$\ln 2/2 \approx 0.35$ h^{-1}	half life = 2 hours
μ_s	$\ln 2/1.9 \times 3600 \approx 1.313 \times 10^3$ h^{-1}	half life = 1.9 seconds
λ_{15}	6.6×10^4 M^{-1} s^{-1}	$= \lambda_{11}$

reactions) to hours (diffusion), which makes numerical computations of the model very slow. Under the space and time scales considered in burn propagation, we simplified our model by using nondimensionalization and assuming quasi-steady-state conditions for the five free radicals (see SI). This simplification is justified by a careful numerical comparison of the simplified model and the full model which shows that the solutions are virtually indistinguishable. All our simulations presented in the Results section are performed for the simplified system.

$$\frac{\partial[\mathrm{LH}]}{\partial t} = -\underbrace{\lambda_2[^{\bullet}\mathrm{OH}][\mathrm{LH}]}_{\text{Reaction (2)}} - \underbrace{\lambda_4[\mathrm{LOO}^{\bullet}][\mathrm{LH}]}_{\text{Reaction (4)}} - \underbrace{\lambda_5[\mathrm{LO}^{\bullet}][\mathrm{LH}]}_{\text{Reaction (5)}}, \tag{1}$$

$$\begin{aligned}\frac{\partial[\mathrm{LOO}^{\bullet}]}{\partial t} = {} & \underbrace{D_{\mathrm{LOO}^{\bullet}}\nabla^2[\mathrm{LOO}^{\bullet}]}_{\text{Diffusion}} + \underbrace{k_3[\mathrm{L}^{\bullet}] + k_7[\mathrm{LOOH}]}_{\text{Reaction (3), (7)}} - \\ & \underbrace{\lambda_4[\mathrm{LH}][\mathrm{LOO}^{\bullet}]}_{(4)} - 2\underbrace{\lambda_9([\mathrm{LOO}^{\bullet}])^2}_{(9)} - \\ & \underbrace{\lambda_{12}[\mathrm{L}^{\bullet}]([\mathrm{LOO}^{\bullet}])}_{(12)} - \underbrace{\lambda_{13}[\mathrm{TocOH}][\mathrm{LOO}^{\bullet}]}_{(13)} - \\ & \underbrace{\lambda_{14}[\mathrm{TocO}^{\bullet}][\mathrm{LOO}^{\bullet}]}_{(14)},\end{aligned} \tag{2}$$

$$\begin{aligned}\frac{\partial[\mathrm{LOOH}]}{\partial t} = {} & \underbrace{D_{\mathrm{LOOH}}\nabla^2[\mathrm{LOOH}]}_{\text{Diffusion}} + \underbrace{\lambda_4[\mathrm{LOO}^{\bullet}][\mathrm{LH}]}_{\text{Reaction (4)}} + \\ & \underbrace{\lambda_{13}[\mathrm{TocOH}][\mathrm{LOO}^{\bullet}]}_{\text{Reaction (13)}} - \underbrace{(k_6 + k_7 + k_8)[\mathrm{LOOH}]}_{\text{Reaction (6), (7), (8)}},\end{aligned} \tag{3}$$

$$\begin{aligned}\frac{\partial[\mathrm{TocOH}]}{\partial t} = {} & \underbrace{D_{\mathrm{TocOH}}\nabla^2[\mathrm{TocOH}]}_{\text{Diffusion}} + \underbrace{k_{a1}}_{\text{Diet}} + \underbrace{k_{a2}}_{\text{Treatment}} - \\ & \underbrace{\lambda_{13}[\mathrm{TocOH}][\mathrm{LOO}^{\bullet}]}_{\text{Reaction (13)}} - \mu_a[\mathrm{TocOH}],\end{aligned} \tag{4}$$

$$\begin{aligned}\frac{\partial[\mathrm{TocO}^{\bullet}]}{\partial t} = {} & \underbrace{D_{\mathrm{TocO}^{\bullet}}\nabla^2[\mathrm{TocO}^{\bullet}]}_{\text{Diffusion}} + \underbrace{\lambda_{13}[\mathrm{TocOH}][\mathrm{LOO}^{\bullet}]}_{\text{Reaction (13)}} - \\ & \underbrace{\lambda_{14}[\mathrm{TocO}^{\bullet}][\mathrm{LOO}^{\bullet}]}_{\text{Reaction (14)}} - 2\lambda_{15}[\mathrm{TocO}^{\bullet}]^2,\end{aligned} \tag{5}$$

$$\begin{aligned}\frac{\partial[^{\bullet}\mathrm{OH}]}{\partial t} = {} & \underbrace{D_{^{\bullet}\mathrm{OH}}\nabla^2[^{\bullet}\mathrm{OH}]}_{\text{Diffusion}} + k_8[\mathrm{LOOH}] - \\ & \lambda_2[^{\bullet}\mathrm{OH}][\mathrm{LH}] - \mu_8[^{\bullet}\mathrm{OH}],\end{aligned} \tag{6}$$

$$\begin{aligned}\frac{\partial[\mathrm{L}^{\bullet}]}{\partial t} = {} & \underbrace{D_{\mathrm{L}^{\bullet}}\nabla^2[\mathrm{L}^{\bullet}]}_{\text{Diffusion}} + \lambda_2[^{\bullet}\mathrm{OH}][\mathrm{LH}] + \lambda_4[\mathrm{LOO}^{\bullet}][\mathrm{LH}] + \\ & \lambda_5[\mathrm{LO}^{\bullet}][\mathrm{LH}] - k_3[\mathrm{L}^{\bullet}] - 2\lambda_{10}[\mathrm{L}^{\bullet}]^2 - \lambda_{12}[\mathrm{L}^{\bullet}][\mathrm{LOO}^{\bullet}],\end{aligned} \tag{7}$$

$$\begin{aligned}\frac{\partial[\mathrm{LO}^{\bullet}]}{\partial t} = {} & \underbrace{D_{\mathrm{LO}^{\bullet}}\nabla^2[\mathrm{LO}^{\bullet}]}_{\text{Diffusion}} + (k_6 + k_8)[\mathrm{LOOH}] - \\ & \lambda_5[\mathrm{LO}^{\bullet}][\mathrm{LH}] - 2\lambda_{11}[\mathrm{LO}^{\bullet}]^2.\end{aligned} \tag{8}$$

Finite difference methods are used to solve the reaction–diffusion system. More specifically, second-order central difference is used for spatial discretization, and semi-implicit schemes are used for the time discretization (see SI). Adaptive small time steps are used for accuracy and stability.

RESULTS

Comparison with a brass comb model of burn: two-dimensional (2-D) simulations

In Singer et al.,[31] an experimental porcine model to study burn damage was designed. Their model used a 20 mm × 20 mm × 50 mm × brass comb with four 10 mm × 20 mm prongs separated by three 5-mm notches that produces four distinctive burn sites separated by three interspaces of unburned skin (refer to Figure 1 in [31]). The brass comb was preheated in boiling water (100°C) for 5 minutes and applied without pressure on one side of the back of the pig for a period of 30 seconds, resulting in four full-thickness burns separated by three unburned interspaces (see Figure 2 in [31]). The interspaces are not directly injured, but within hours, they undergo progressive ischemia, and, at 24 to 48 hours, they become necrotic.

We compare our model with the experimental results of Singer et al., by comparing the burn propagation along the surface of the skin. In order to establish "proof of concept" of our model, we first assumed that all the chemicals do not vary much over the depth of the wound, and therefore simulated the model for geometry of the brass comb in the 2-D case. This assumption can also be thought as averaging all the variables over the depth of the wound- therefore, we used the same diffusion rates as in the three-dimensional (3-D) case.

Figure 3A depicts the 2-D geometry of the brass comb; the initial burn is confined to the four rectangular regions. Figure 3B shows the numerical solution of the concentrations of lipid and lipid peroxide 12 hours after the initial burn. The parameters used in our simulations are based on Tables 1 and 2, and the simulated physical time is 12 hours. The simulations are performed in a large rectangle (7 cm in the x-direction and 3 cm in the y-direction) which contains all the four small rectangles. We use no-flux boundary conditions for all the species on the four boundaries of the rectangular computational domain ($-3.5 \le x \le 3.5$, $-1.5 \le y \le 1.5$). We assume that initially, in the burn area, [LH] = 0, [TocOH] = 0, [LOOH] = 0, and in the healthy area, [LH] = L_0, [TocOH] = A_0, [LOOH] = 0, with all the other initial species solved by the quasi-steady-state assumptions. The tissue in the interspace between rectangles clearly suffered excessive

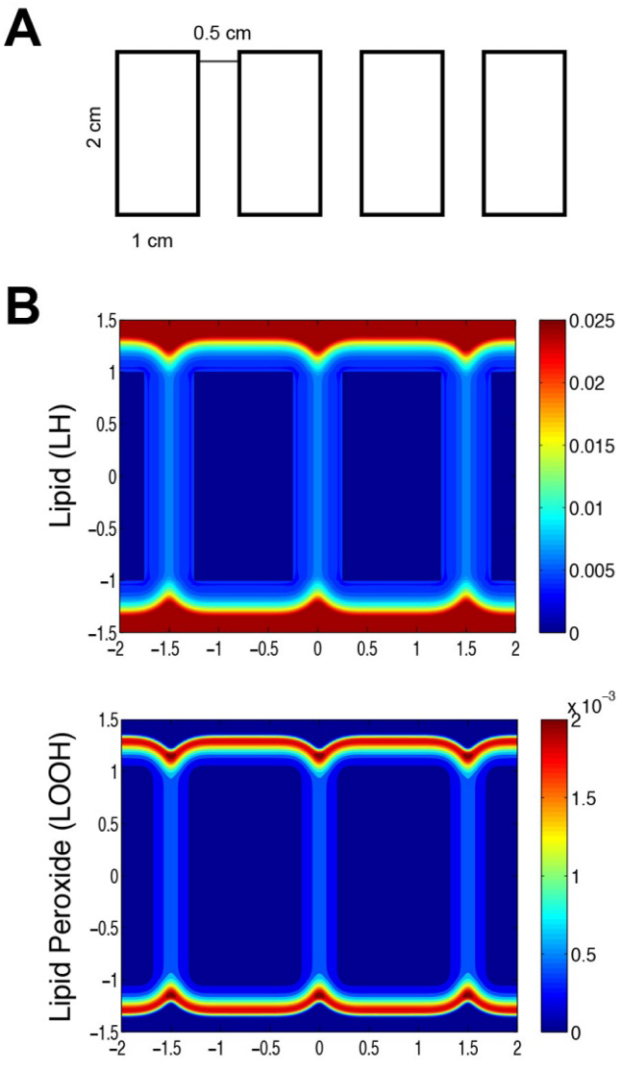

Figure 3. Two-dimensional simulation for brass comb model of a burn at 12 hours after the initial heat shock. (A) Two-dimensional surface view of the geometry of brass comb burn. (B) Contours of concentrations of lipid (L) and lipid peroxide (P) (zoomed in for viewing the interspace areas), with color bars displaying the levels of these species; the interspace between the original burn area is where the ischemia occurs, and this simulation is using k_{a1} with values 10 times lower in the interspaces than in other areas.

vascular damage by the burn. We account for this by decreasing the replenish rate of the natural vitamin E, k_{a1}, in the interspace between the rectangles by a factor of 10. Although it is not possible to exactly compare the profiles in Figure 3B to tissue damage shown in the experiments of Singer et al., the progression of the burn in the simulation and the experiments show the same pattern.

The effect of vitamin E intervention: 3-D simulations

We simulated the burn wounds in 3-D space, without intervention and with intervention by vitamin E, i.e., $k_{a2} = 0$ and $k_{a2} = 5k_{a1}$. The goal was to test, by the mathematical model, the efficacy of vitamin E in slowing down the lipid peroxide propagation. For simplicity, we assumed that the epidermal layer and the dermal layer are both homogeneous and parallel to the horizontal plane. Although the diffusion rates of the chemical species in the epidermal layer may be smaller than that of the dermal layer, for simplicity, we take them to be the same. We also assume, for simplicity, that the initial wound is restricted within the pink cube with $-0.5 \le x \le 0.5$, $-0.5 \le y \le 0.5$, $-1 \le z \le 0$, and take the computational domain to be $-1 \le x \le 1$, $-1 \le y \le 1$, $-2 \le z \le 0$, as illustrated in Figure 4.

The initial conditions were taken by assuming that the initial damage is proportional to the temperature of the tissue after the burn. More specifically, we assumed that at the initial instant, $U = 0$ in the burned area, and $U = 1$ elsewhere, and solved the equation

$$\frac{\partial U}{\partial t} = D_U \nabla^2 U,$$

in the pink region in Figure 4 during the burning, with $D_U = 1\ \mathrm{cm^2 h^{-1}}$, and the boundary conditions

$$U(x, y, 0) = 0, U(x, y, -1) = U(-0.5, y, z) = U(0.5, y, z) = U(x, -0.5, z) = U(x, 0.5, z) = 1.$$

We further define $U = 1$ outside the burned area, and then take 1-U to represent the temperature distribution immediately after the burn. To incorporate the temperature effect of the initial burn, which has contact only on the surface of the skin $z = 0$, we take the following initial conditions for the various species to be

$$[\mathrm{LH}] = L_0 U, [\mathrm{TocOH}] = A_0 U, [\mathrm{LOOH}] = P_0(1 - U),$$

where U is the temperature at the end of the burning, i.e., $t = 30$ seconds.

Under the above-described 3-D scenario, the dynamics of the lipid and lipid peroxide are shown in Figure 5A and B, respectively, with both top view and side view at time 1, 6, and 12 hours. The parameters are taken as in Tables 1 and 2 unless otherwise noted. In order to quantitatively analyze the propagation of the burn wound, we tracked the location where the lipid concentration is 90% of its maximum, and use it to quantify the size of the damage in Figure 5C. We note that this criterion gives similar result by using the peak of the lipid peroxide concentration. We found that the progression of damage without vitamin E intervention is rapid, having increased 20% in the xy-direction and 20% in xz-direction in 12 hours. However, with vitamin E treatment, the resulting propagation of the burn wound at time 1, 6, and 12 hours is reduced to 10%. Figure 5C shows that the size of the wound increases approximately linearly in these 12 hours, with or without vitamin E, and the rate of propagation of the burn wound with vitamin E treatment is about 50% of that without vitamin E treatment. As we did not take into account different compositions of the skin layers, and also assumed that the propagation speed in the horizontal direction and in the vertical direction do not vary. The propagation speed predicted from our simulation is probably more rapid than what has been observed in clinics because we did not consider the effect of the heterogeneous complex

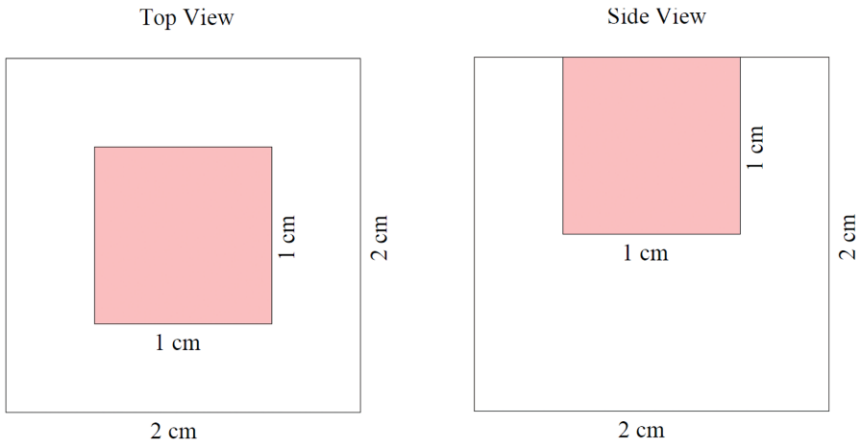

Figure 4. Illustration of the three-dimensional computational domain.

composition of the skin, which can potentially slow down the diffusion of the chemicals. The propagation may slow down afterwards, as the reparative processes of wound healing may take over.

We compared the numerical results with those performed in a larger computational domain (not shown here) and found that the solutions near the initial burn are virtually indistinguishable. This confirms that there is no boundary effect for the computational domain used here.

Sensitivity analysis

We have performed Partial Rank Correlation Coefficient (PRCC) sensitivity analysis[35] for the burn propagation at $T = 12$ in 2-D simulations on 19 parameters. The 2-D simulations are based on the assumption of homogeneity in the z-direction of the 3-D model.

We estimated the expansion of the wound along the x-axis. The region of the wound is defined as the region where the lipid concentration is less than 90% of that of the healthy tissue. Latin hypercube sampling method was used to sample the parameters. The range of each parameter is chosen as 0.5 to 1.5 times the values listed in Tables 1 and 2. Each range is divided into 1,000 intervals of uniform length. Each interval for each parameter is sampled exactly once (without replacement), so that the entire range of each parameter is explored. Table 3 summarizes the PRCC values and p-values for these 19 parameters (see Supporting Information Figure S1). The significant parameters are those parameters that have p-value less than 0.01. We found that the following parameters D_{LOOH} (diffusion rate of lipid peroxide), μ_a (degradation rate for vitamin E), λ_4 (reaction rate of LOO$^\bullet$ to lipid) are highly positively correlated, while k_{a1} (growth rate for vitamin E from diet) and λ_9 (degradation rate for LOO$^\bullet$) are highly negatively correlated. The results are consistent with the intuition that the faster the lipid peroxide diffuses, the faster the burn propagates; and, similarly, the faster vitamin E degrades, or the slower vitamin E from diet is absorbed, or the slower LOO$^\bullet$ degrades, the faster the burn is expected to propagate.

We further investigated the effectiveness of vitamin E treatment against the uncertainties of the parameters (Figure 6). The results show that five times topical vitamin E treatment can slow down the propagation of burn on average by at least 50%, and this prediction is quite robust for a large range of randomly chosen parameters.

Table 3. PRCC sensitivity analysis

Parameters	PRCC (p-value)
D_{LOOH}	0.91211 (0)
D_{TocOH}	–0.11037 (4.7162e-04)
k_{a1}	–0.83987 (<<1.e-4)
k_3	–0.025615 (0.41844)
k_6	0.47569 (<<1.e-4)
k_7	0.58658 (<<1.e-4)
k_8	0.19888 (<<1.e-4)
μ_a	0.74742 (<<1.e-4)
μ_s	–0.037993 (0.22999)
λ_2	–0.032165 (0.30957)
λ_4	0.93173 (0)
λ_5	0.025118 (0.42753)
λ_9	–0.76215 (<<1.e-4)
λ_{10}	0.01816 (0.56623)
λ_{11}	0.016474 (0.60283)
λ_{12}	–0.028103 (0.37467)
λ_{13}	–0.024296 (0.44282)
λ_{14}	–0.04696 (0.13782)
λ_{15}	0.037622 (0.23457)

DISCUSSION

The skin, especially the surface, is packed with lipids. Immediately after skin burn injury has occurred, the tissue damage propagates as a result of a series of chemical reactions of lipid-centered radicals, and this propagation may persists for more than 12 hours. These reactions result in accumulation of reactive oxygen and lipid species and depletion of lipid-phase antioxidants in the tissue, which cause the tissue deterioration. After 12 hours of burn, infiltrating neutrophils may exaggerate the situation by

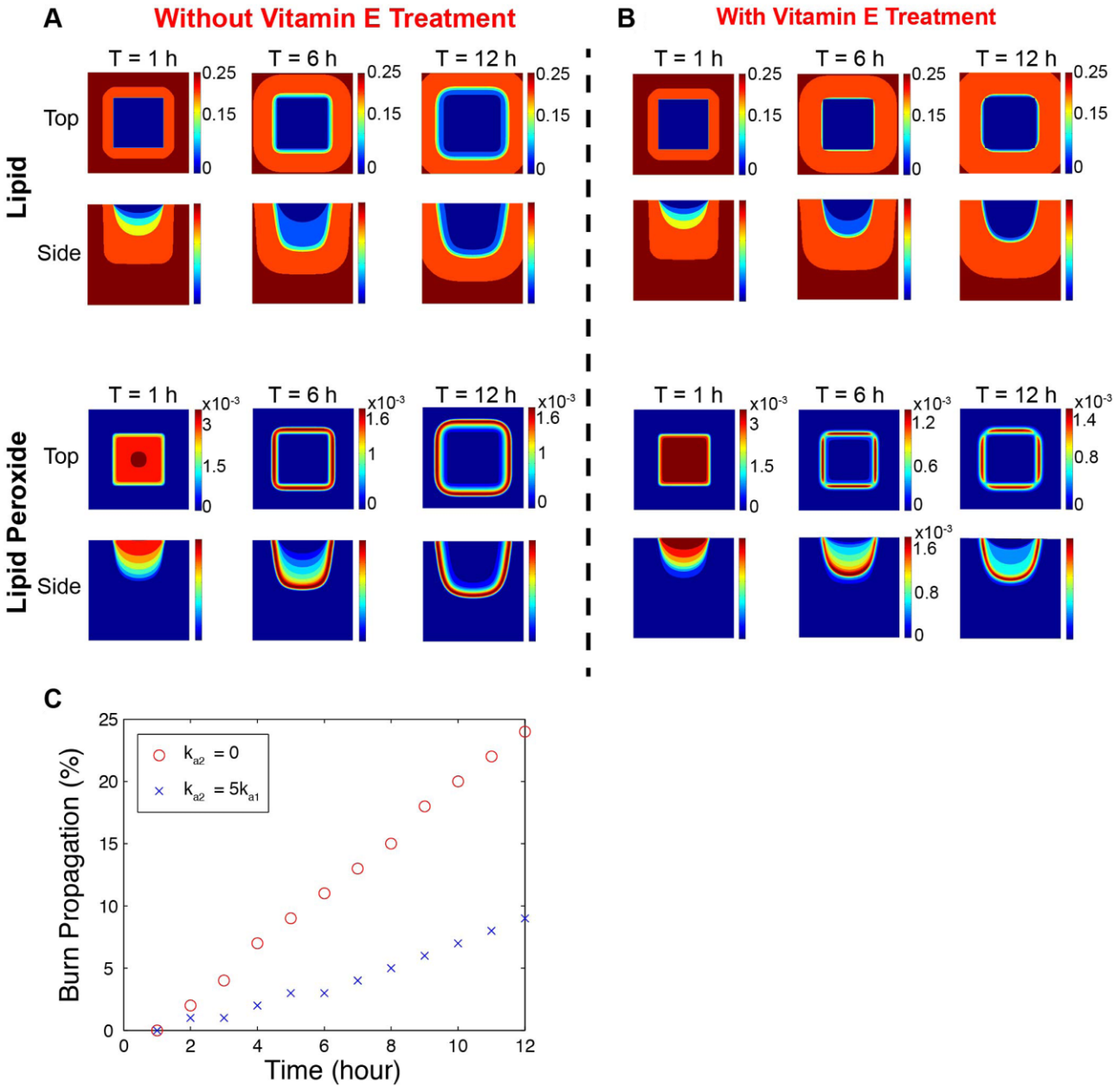

Figure 5. Three-dimensional simulations of the burn wound at 1, 6, and 12 hours after the initial heat shock. (A) Without vitamin E treatment ($k_{a2} = 0$), distributions lipid (L) and lipid peroxide (P); the upper panels (top view) display the contours of distributions of those species at $z = 0$, and the lower panels (side view) display the contours of distributions of species at $y = 0.5$. (B) With vitamin E treatment ($k_{a2} = 5k_{a1}$). Color bars beside the contours indicate the levels of the species, and the scales of the top view and side view are the same unless otherwise indicated. (C) The percentage of burn wound propagation with respect to time are shown for $k_{a2} = 0$ and $k_{a2} = 5k_{a1}$, respectively. The size of the burn wound with vitamin E treatment is about half of the size of that without vitamin E treatment.

contributing more ROS to the wound site as part of "respiratory-burst" process.

This paper develops a novel 3-D mathematical description on the propagation of tissue damage within 12 hours after a burn, when neutrophils function at the wound site may be considered to be present but negligible for the purposes of our mathematical modeling. The current model is based on the lipid peroxidation chain reactions that take place immediately after thermal wound injury. It is formulated in terms of a system of partial differential equations that incorporate the

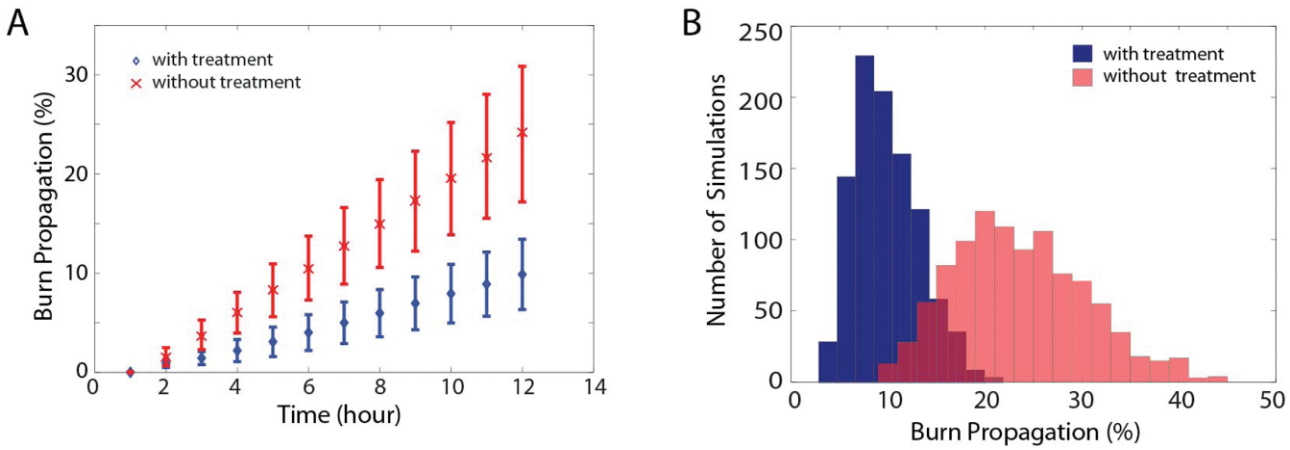

Figure 6. Statistics of 1,000 simulations with randomly selected parameters, for burn wound propagation, with and without vitamin E treatment. The parameter k_{a1} is a random variable in an interval which contains the natural production rate of vitamin E, 1.4×10^{-4} Mh^{-1}. For the untreated cases, we take $k_{a2} = 0$, and, for the treated cases, we take $k_{a2} = 5 \times 1.4 \times 10^{-4}$ Mh^{-1}. (A) Time history of the burn propagation. The marks "x" and "◇" stand for the mean of the burn propagation over 1,000 simulations at each time, and the bars for the standard deviation. (B) Histograms of the statistics at $T = 12$ for treated (blue) and untreated (red) cases.

chemical reactions using mass action kinetics and the diffusion of the chemical species in the tissue surrounding the wound. The various rate parameters are obtained from the experimental literature. The 3-D formulation is readily applicable to dermal injuries (partial-thickness or second-degree burns). Simulations for comb burns show qualitative agreement with documented experimental measurements.

The mathematical model was used to investigate the effect of treatment with vitamin E. We simulated the wound burn propagation with and without vitamin E treatment, and found that vitamin E treatment can substantially reduce lipid peroxide propagation for partial-thickness burn wounds. We have assumed that, to simplify the computation, the tissue surrounding the wound is homogeneous. The heat propagation is incorporated through the initial conditions that reflect the dermal damage caused initially by the burn.

The main interest of this paper is to show how tissue damage propagates in the first 12 hours after the initial burn injury. As mentioned above, few neutrophils come to the burned area during this period of time. After this initial period, neutrophils deliver ROS and exaggerate the oxidative stress. Other reparative processes of wound healing may also be initiated. Therefore, in order to get a quantitative understanding of the dynamics of lipid peroxide concentration, one needs to incorporate these factors into the mathematical model, which is left as future work.

Based on the present model, we hypothesize that vitamin E can substantially reduce tissue damage propagation for partial-thickness burns immediately after the initial injury. To the extent that this hypothesis is biologically confirmed, and further development of the model includes experimental data based on temperature measurements, the model could become a predictive tool for the determination of the size and depth of tissue damage, as well as for predicting the results of treatments of cutaneous burn wounds.

ACKNOWLEDGMENTS

The project described was supported by Award Number UL1RR025755 from the National Center for Research Resources. The content is solely the responsibility of the authors and does not necessarily represent the official views of the National Center for Research Resources or the National Institutes of Health. This research has been supported in part by the Mathematical Biosciences Institute and the National Science Foundation under grant DMS 0931642. The work is also supported in part by GM069589 and GM077185 from National Institute of General Medical Sciences (NIGMS) to CKS, and NSF grant DMS1020625 to CSC.

REFERENCES

1. Nguyen TT, Gilpin DA, Meyer NA, Herndon DN. Current treatment of severely burned patients. *Ann Surg* 1996; 223: 14–25.
2. Gutteridge J. Lipid peroxidation and antioxidants as biomarkers of tissue damage. *Clin Chem* 1995; 41: 1819–28.
3. Doktorov AB, Lukzen NN, Pedersen JB. Analysis of lipid peroxidation kinetics. 1. Role of recombination of alkyl and peroxyl radicals. *J Phys Chem B* 2008; 112: 11854–61.
4. http://en.wikipedia.org/wiki/Lipid_peroxidation.
5. Latha B, Babu M. The involvement of free radicals in burn injury: a review. *Burns* 2001; 27: 309–17.
6. Halliwell B, Gutteridge JMC. *Free radicals in biology and medicine*, 4th ed. Oxford: Oxford University Press, 2007.
7. Logani MK, Davies RE. Lipid oxidation: biologic effects and antioxidants—a review. *Lipids* 1980; 15: 485–95.
8. Sevanian A, Hochstein P. Mechanisms and consequences of lipid peroxidation in biological systems. *Annu Rev Nutr* 1985; 5: 365–90.
9. Frankel EN. Recent advances in lipid oxidation. *J Sci Food Agric* 1991; 54: 495–511.

10. Catalá A. A synopsis of the process of lipid peroxidation since the discovery of the essential fatty acids. *Biochem Biophys Res Commun* 2010; 399: 318–23.
11. Negre-Salvayre A, Auge N, Ayala V, Basaga H, Boada J, Brenke R, Chapple S, Cohen G, Feher J, Grune T, Lengyel G, Mann GE, Pamplona R, Poli G, Portero-Otin M, Riahi Y, Salvayre R, Sasson S, Serrano J, Shamni O, Siems W, Siow RC, Wiswedel I, Zarkovic K, Zarkovic N. Pathological aspects of lipid peroxidation. *Free Radic Res* 2010; 44: 1125–71.
12. Naumov AA, Shatalin YV, Potselueva MM. Effects of a nanocomplex containing antioxidant, lipid, and amino acid on thermal burn wound surface. *Bull Exp Biol Med* 2010; 149: 62–6.
13. Bekyarova G, Galunska B, Ivanova D, Yankova T. Effect of melatonin on burn-induced gastric mucosal injury in rats. *Burns* 2009; 35: 863–8.
14. Bekyarova G. Yankova T. alpha-Tocopherol and reduced glutathione deficiency and decreased deformability of erythrocytes after thermal skin injury. *Acta Physiol Pharmacol Bulg* 1998; 23: 55–9.
15. Bekyarova G, Yankova T, Kozarev I. Suppressive effect of FC-43 perfluorocarbon emulsion on enhanced oxidative haemolysis in the early postburn phase. *Burns* 1997; 23: 117–21.
16. Bekyarova G, Yankova T, Kozarev I. Combined application of alpha-tocopherol and FC-43 perfluorocarbon emulsion suppresses early postburn lipid peroxidation and improves deformability of erythrocytes. *Acta Chir Plast* 1998; 40: 17–21.
17. Bekyarova G, Yankova T, Kozarev I, Yankov D. Reduced erythrocyte deformability related to activated lipid peroxidation during the early postburn period. *Burns* 1996; 22: 291–4.
18. Phan TT, See P, Lee ST, Chan SY. Protective effects of curcumin against oxidative damage on skin cells in vitro: its implication for wound healing. *J Trauma* 2001; 51: 927–31.
19. Hortan JW. Free radicals and lipid peroxidation mediated injury in burn trauma: the role of antioxidant therapy. *Toxicology* 2003; 189: 75–88.
20. Panin G, Strumia R, Ursini F. Topical alpha-tocopherol acetate in the bulk phase: eight years of experience in skin treatment. *Ann N Y Acad Sci* 2004; 1031: 443–7.
21. Mustacich DJ, Bruno RS, Traber MG. Vitamin E. *Vitam Horm* 2007; 76: 1–21.
22. Parihar A, Parihar MS, Milner S, Bhat S. Oxidative stress and anti-oxidative mobilization in burn injury. *Burns* 2008; 34: 6–17.
23. Traber MG, Leonard SW, Traber DL, Traber LD, Gallagher J, Bobe G, Jeschke MG, Finnerty CC. Herndon D. α-Tocopherol adipose tissue stores are depleted after burn injury in pediatric patients. *Am J Clin Nutr* 2010; 92: 1378–84.
24. Sen CK, Khanna S, Rink C, Roy S. Tocotrienols: the emerging face of natural vitamin E. *Vitam Horm* 2007; 76: 203–61.
25. Sen CK, Khanna S, Roy S. Tocotrienols: vitamin E beyond tocopherols. *Life Sci* 2006; 78: 2088–98.
26. Sen CK, Khanna S, Roy S. Tocotrienols in health and disease: the other half of the natural vitamin E family. *Mol Aspects Med* 2007; 28: 692–728.
27. Diegelmann RF, Evans MC. Wound healing: an overview of acute, fibrotic and delayed healing. *Front Biosci* 2004; 9: 283–9.
28. Liu KC. Thermal propagation analysis for living tissue with surface heating. *Int J Therm Sci* 2008; 47: 507–13.
29. Dai W, Wang H, Jordan PM, Mickens RE, Bejan A. A mathematical model for skin burn injury induced by radiation heating. *Int J Heat Mass Transf* 2008; 51: 5497–510.
30. Ng EYK, Chua LT. Comparison of one- and two-dimensional programmes for predicting the state of skin burns. *Burns* 2002; 28: 27–34.
31. Singer AJ, McClain SA, Taira BR, Romanov A, Rooney J, Zimmerman T. Validation of a porcine comb burn model. *Am J Emerg Med* 2009; 27: 285–8.
32. Reddanna P, Rao MK, Reddy CC. Inhibition of 5-lipoxygenase by vitamin E. *FEBS Lett* 1985; 193: 39–43.
33. German JB, Kinsella JE. Lipid oxidation in fish tissue. Enzymic initiation via lipoxygenase. *J Agric Food Chem* 1985; 33: 680–3.
34. http://en.wikipedia.org/wiki/Lipoxygenase.
35. Marino S, Hogue IB, Ray CJ, Kirschner DE. A methodology for performing global uncertainty and sensitivity analysis in systems biology. *J Theor Biol* 2008; 254: 178–96.
36. Antunes F, Salvador A, Marinho HS, Alves R, Pinto RE. Lipid peroxidation in mitochondrial inner membranes. I. An integrative kinetic model. *Free Radic Biol Med* 1996; 21: 917–43.
37. Barber DJW, Thomas JK. Reactions of radicals with lecithin bilayers. *Radiat Res* 1978; 74: 51–65.
38. Belitz HD, Grosch W. *Food chemistry*, 2nd ed. Berlin: Springer, 1999.
39. Barclay LRC, Baskin KA, Locke SJ, Vinqvist MR. Absolute rate constants for lipid peroxidation and inhibition in model biomembranes. *Can J Chem* 1989; 67: 1366–9.
40. Vaz WLC, Goodsaid-Zalduondo F, Jacobson K. Lateral diffusion of lipids and proteins i Jn bilayer membranes. *FEBS Lett* 1984; 174: 199–207.
41. Aranda F, Coutinho A, Berberan-Santos M, Prieto M, Gomez-Fernandez J. Fluorescence study of the location and dynamics of [alpha]-tocopherol in phospholipid vesicles. *Biochim Biophys Acta (BBA)-Biomembranes* 1989; 985: 26–32.
42. Alexander-North LS, North JA, Kiminyo KP, Buettner GR, Spector AA. Polyunsaturated fatty acids increase lipid radical formation induced by oxidant stress in endothelial cells. *J Lipid Res* 1994; 35: 1773–85.

Supporting Information

Additional Supporting Information may be found in the online version of this article:

Figure S1. PRCC sensitivity analysis for the burn propagation at $T = 12$ in two-dimensional simulations on 19 parameters. PRCC values and p-values for these 19 parameters are listed on the top of each subfigure. We found that the following parameters D_{LOOH}, μ_a, λ_4 are highly positively correlated while the parameters k_{a1}, λ_9 are highly negatively correlated.

Please note: Wiley-Blackwell is not responsible for the content or functionality of any supporting materials supplied by the authors. Any queries (other than missing material) should be directed to the corresponding author for the article.